Segmentation of Nuclei in Histopathology images using Fully Convolutional Deep Neural Architecture

Conference Paper · September 2020

DOI: 10.1109/ICCIT-144147971.2020.9213817

5 authors, including:

V. Anantha Natarajan
Sree Vidyanikethan Engineering College
6 PUBLICATIONS **49** CITATIONS
SEE PROFILE

M. Sunil Kumar
Sree Vidyanikethan Engineering College
49 PUBLICATIONS **254** CITATIONS
SEE PROFILE

Rizwan Patan
Galgotias University
85 PUBLICATIONS **1,312** CITATIONS
SEE PROFILE

Suresh Kallam
Galgotias University
32 PUBLICATIONS **231** CITATIONS
SEE PROFILE

2020 International Conference on Computing and Information Technology, University of Tabuk, Kingdom of Saudi Arabia.
Volume: 01, Issue: ICCIT- 1441, Page No.: 319 – 325, 9th & 10th Sep. 2020.

Segmentation of Nuclei in Histopathology images using Fully Convolutional Deep Neural Architecture

V. Anantha Natarajan[1], M. Sunil Kumar[1], Rizwan Patan[2], Suresh Kallam[1], Mohamed Yasin Noor Mohamed[3]
[1]Department of Computer Science and Engineering, Sree Vidyanikethan Engineering College, Tirupati, India
[2]Department of Computer Science and Engineering, Velagapudi Ramakrishna Siddhartha Engineering College, Vijayawada, India
[3]Department of Math and IT, Center for Preparatory Studies, Sultan Qaboos University, Muscat, Sultanate of Oman
vananthanatarajan@vidyanikethan.edu, sunilmalchi@vidyanikethan.edu, prizwan5@gmail.com, sureshkallam@vidyanikethan.edu, yascrescent@gmail.com

***Abstract*— Nuclei segmentation is an initial step in the automated analysis of digitized microscopic images. This paper focuses on utilizing the LinkNET-34 architecture for semantic segmentation of nuclei from the H&E stained breast cancer histopathology images. The segmentation process is implemented in two stages where in the first stage the H&E stained images are pre-processed to reduce the variance caused because of staining the microscopic images and scanning the slides. During the second stage the pre-processed images are given as input to the LinkNET network which consists of both down-sampling and up-sampling layers. The network is trained using a set of WSI patches released during the Data Science bowl 2018 competition. The performance of the deep learning model is evaluated based on the segmentation accuracy measured using the Dice Co-efficient.**

Keywords: nuclei segmentation; breast cancer; LinkNet-34; histopathology images; WSI patches; Dice Co-efficient

I.INTRODUCTION

Invasive Ductal Carcinoma (IDC) also known as infiltrating Ductal Carcinoma is the most well-known kind of breast cancer and 80% of breast cancer in women is classified as IDC. The term invasive is used to denote the growth of cancer cells up to surroundings of the breast tissues. Ductal refers to the fact that the cancer started growing in the pipes (aka ducts) which carries milk from the lobules. The name Carcinoma applies to any type of cancer that started growing from skin or tissues. On a whole the IDC refers to the cancer that has originated from the walls of the milk ducts and infiltrated to surrounding breast tissues. As time grows the cancer can grow up to the lymph nodes and other parts of the body.

Breast Cancer ranks top in the list of cancer among females in India with a high Age Adjusted Rate (AAR) of 25.8 per 100, 000 women and mortality rate of 12.7 per 100,000 women in India [1]. The study collected reports and data from various cancer registries in the country and analyzed the incidence and mortality rates. The mortality to incidence ration for regular registered cases was observed to be 66 and availability better diagnosis and treatment method might create a healthy living condition within the country. In Table 1. the ranking of the Indian cities based on different rates of cancer is presented. The Computer Aided Diagnosis (CAD) can help the radiologist in better diagnosing the cancer in the very early stage of the disease. The CAD system will help the physician in discriminating the normal tissues from the diseased or abnormal tissues. It should be noted that a CAD system cannot substitute a physician but it can be good supplement in the diagnosis process.

The conventional methods used by the pathologists for the analysis of the cancerous tissues are histological grade determination, and finding the hormone receptor status using Immuno-Histo-Chemistry (IHC) [3]. These complex methods and the results are not accurate due to the variation in the observer [4]. The IHC stained glass slides are used to estimate the volume of positive cells for a given antigen and the degree of staining intensity. Whole Slide Imaging (WSI) scanners are considered to be the successors of the microscope attached digital cameras. The WSI emulates the microscopic investigation by a digital approach where advanced scanners used to digitize the glass slides [17]. The digital slides can be processed or analyzed further using sophisticated tools and software. The WSI's are high resolution images which provide a scope for developing CAD and analysis techniques.

Table 1 Ranking and rates for breast cancer

Breast	%†	R‡	CR§per 100 000	AAR* per 100 000
Mumbai	28.8	1	33.6	33.6
Bangalore	27.5	1	29.3	34.4
Chennai	30.7	1	40.6	37.9
Thiruvanantha puram	28.5	1	43.9	33.7
Dibrugarh	19	1	12.7	13.9
New Delhi	28.6	1	34.8	41
Barshi Rural	20	2	13.2	12.4

†Relative proportion.
‡Rank.
§Crude rate.
*Age adjusted rate.

The biological tissues have a complex structure and the structure of a healthy tissue greatly varies from one person to another. Similarly the structure of a diseased tissue also varies between individuals having the same disease. The automated analysis of the WSI images are more challenging due to this variance and the high resolution property of them [5]. In medical diagnosis the WSI's are stained as most of the cells are transparent and color-less in nature. Hematoxylin & Eosin (H&E)

978-1-7281-2680-7/20/$31.00 ©2020 IEEE

staining is majorly used procedure in histopathological analysis of breast cancer. This staining provides a good view of the effects of the disease on cells of the tissues.

The hemotoxylin stains the nuclei of the cell with blue and purple color and the eosin stains the cytoplasm of the cell and the connective tissues with pink color. The Figure 1 shows a sample H&E stained breast cancer images. The following challenges are identified in the cell nuclei segmentation i. Variance in H&E stained images introduced during the image acquisition itself. ii. Uneven intensities of the non-nuclei region which makes the discrimination of nuclei and non-nuclei region harder. iii. Merged and overlapped representation of cell nuclei when 3D structure of tissues is projected in to 2D images.

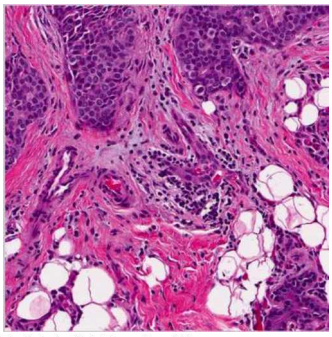

Fig. 1. Sample IDC (+) H&E stained image

This paper focuses on developing deep learning model to segment nuclei present in H&E stained IDC images. The nuclei segmentation is more challenging as its appearance varies greatly when compared with the other organs [18]. The stain absorption, textural and morphological characteristics of the nucleus have more differences. Considering all the heterogeneous characteristics of the nuclei in terms of shape and challenging nature of the H&E images, it is assumed that the deep learning based segmentation can yield better results when compared to conventional handcrafted procedures. The segmentation of nuclei is considered to be an essential as the cancers can be graded based on the morphology of the nucleus. At present many researches have been conducted for nuclei segmentation and they yield promising results.

Experimental results presented in the section 4 demonstrate high segmentation performance with efficient precision, recall and dice-coefficient rates, upon testing high-grade breast cancer images. The deep learning models were trained and tested on WSI and patches of breast cancer histopathology images. The paper is organized as follows. In section 2 the literatures related to bio medical image segmentation using deep learning models and the conventional methods are reviewed. Section 3 presents the description about the dataset and Section 4 describes the methodology used. The section 4 presents the experiments and results. Finally the section 5 concludes the paper.

II.RELATED WORKS

Nuclei segmentation is the initial task carried out in the CAD which determines the overall success of the analysis process. Hence a variety of segmentation based on conventional digital image processing algorithms and deep learning techniques have been proposed in various literatures. The conventional methods either suffer from under or over segmentation problems due to complex and heterogeneous natures of the cell nuclei across images. In some of the literatures the over segmentation problem was handled using region growing method but this method performs poor in segmenting the overlapping cell nuclei [6]. In some of the literature [7] the clustering techniques were applied to the nuclei segmentation problem and the results are not satisfactory as the clustering techniques are sensitive to the variations in the intensity within the nuclei.

In the present research scenario deep learning methods are utilized in segmentation tasks after their successful implementation in many computer vision tasks. The fully connected layers are converted into deep convolutional layers to identify the heatmap of the objects in the image. Mask R-CNN a successor of fast R-CNN, segments an image using a two-stage process [9]. In the first stage the images are scanned and candidate regions that likely contain the objects are identified. Then in the second stage the candidate regions are classified and masks are generated with bounding boxes. Mask R-CNN architecture is complex when compared to other deep learning architectures as both prediction of segmentation masks and bounding-box regression are carried in parallel. From the qualitative analysis of the results of the Mask R-CNN it is observed that it does not generated small extra-nuclear debris but it nucleus pixel recall is low. Recently U-Net, fully convolutional neural network based architecture is used most widely in the field of bio medical image segmentation [8]. The U-Net architecture consists of a contracting and a symmetric expanding path. The network was trained with very few images and the results were better when compared to sliding window convolutional network.

III.METHODOLOGY

The segmentation of the histopathology images requires pre-processing tasks to balance the effects of staining the images. The benchmark dataset considered for training our model is composed of a large volume of segmented nuclei images and image acquisition was done at various conditions, magnification, and brightfield or fluorescence imaging modality. Each binary mask contains one nucleus. The nuclei segments does not overlap when masks are merged together to form a single binary mask. The dataset consist of 694 images scanned at 40x. Across these images there are about 12,000 nuclei manually segmented. The data set is available as a part of the Data Science Bowl 2018 competition [12].

a. Pre-processing of Histopathology Images

The initial step in analysing a bright field microscopic image is color and illumination normalization. The normalization helps to reduce the variance in the tissues

samples caused due to staining and scanning conditions. The illumination variation can be reduced or eliminated by utilizing a target image or by estimation of the illumination pattern using a curve fitting process. Histogram matching can also be used to reduce the illumination variation. The standardization procedure is followed to balance the brightness in the images and then normalized to highlight the difference between the nuclei and other tissue region. The Figure 2 to 5 presents the raw H&E stained images and the results of standardization and normalization process.

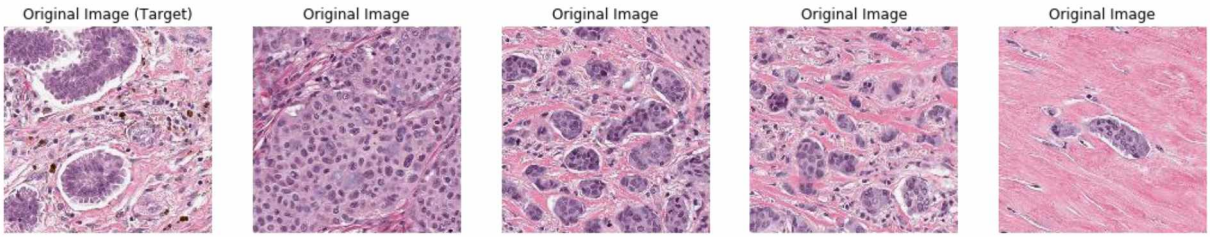

Fig. 2. Raw H&E stained Images

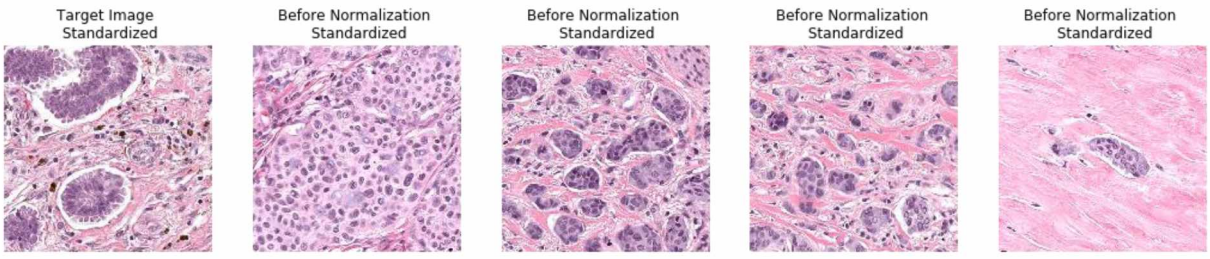

Fig. 3. Brightness Standardized Images

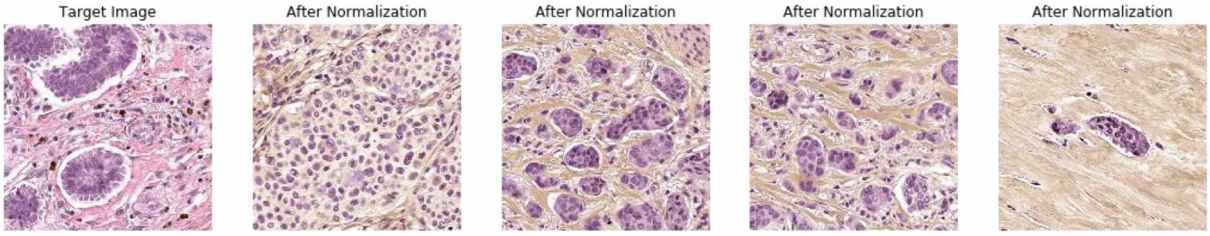

Fig. 4. Normalized H&E stained Images

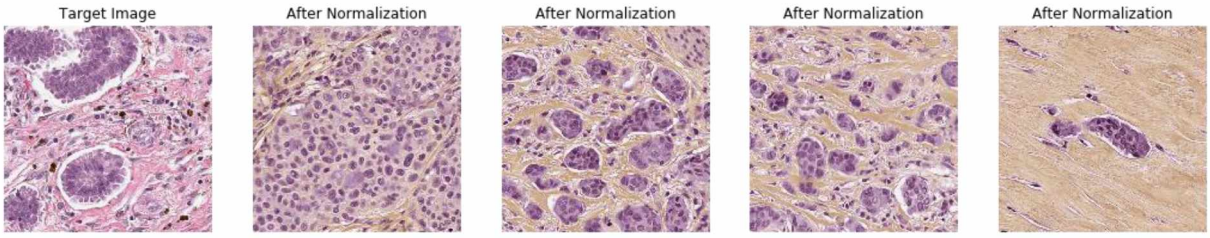

Fig. 5. Normalized Image (without Standardization)

b. Segmentation using LinkNet

The architecture of LinkNET contains a series of blocks of encoder and decoder which respectively break down the image and constructs it back. Final the images are made to pass through few convolutional layers. The design of the model aimed at minimizing the number of parameters which makes the model suitable for real time segmentation tasks.

The LinkNet architecture was derived from the architecture of ResNet [13]. The LinkNet34 architecture used for nuclei segmentation is presented in the Figure 6. The first block of the model performs a convolution on the input image using a 7x7 size kernel with stride of 2. It is followed by a max-pooling layer with a stride of 2. The next set of layers is formed by a series of residual blocks. In each of the residual block the initial convolutional layer will have a stride of 2 doing the downsampling of the input and rest of the convolutional layers in the respective block will have stride of 1. Also the model consists of a series of decoder block which are connected to the respective encoder block. The decoder block does a 1x1 convolution operation which is followed by batch normalization and transposed

convolutions for up sampling the obtained feature maps in the previous blocks.

The architecture of the LinkNET varies greatly from the architecture of the existing neural architectures designed for pixel-wise segmentation. The uniqueness of the LinkNET architecture lies in the connection between the encoder and corresponding decoder block. Usually spatial information is lost during sequence of decoding operation and it is difficult to recover this lost information from the output of the encoder. Through pooling indices the encoder is linked with decoder and these are non-trainable parameters [14]. Some other methods directly link the output of the encoder to the decoder for performing the segmentation. In the LinkNET architecture, a link is established to bypass the input of the encoder and feed it into the output of the decoder. This link is aimed at recovering the lost spatial information due to sequence of encoding operation and used during the upsampling operation by the decoder. As per this architecture the decoder uses few parameters as it is sharing the knowledge learned by the encoder. This architecture helps to build a more efficient network which is suitable for real time operations when compared to the existing architectures used for segmentation [19].

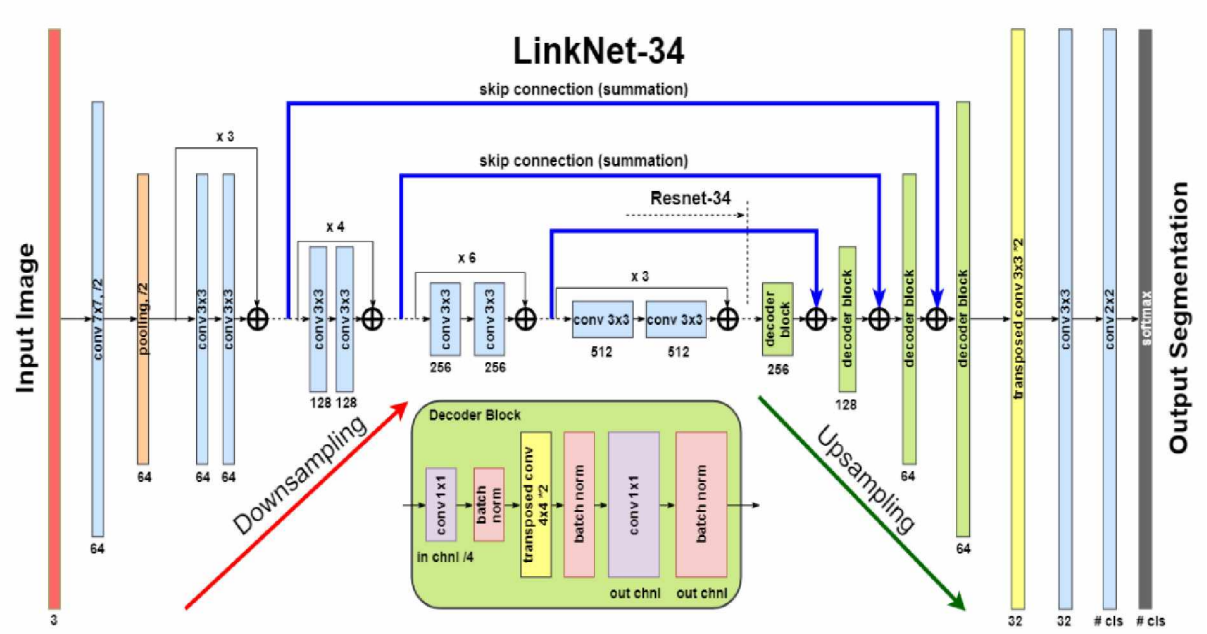

Fig. 6. Schematic view of LinkNET-34's architecture [16]

In biomedical image segmentation the region of interest will be small which makes the model to stick in the local minima during training process. Because of this the predictions of the trained model will be biased towards to the background pixels. In the final results the foreground region will appear to be missing or partially detected. To overcome this issue more importance has to be given to foreground rather background region during the training process. The objective function using Dice Coefficient has such a focus and the value of Dice Coefficient ranges between 0 and 1. The aim is to maximize the Dice Coefficient which is expressed mathematically as shown in Eq. 1

$$D = \frac{2\sum_i^N p_i g_i}{\sum_i^N p_i^2 + \sum_i^N g_i^2} \quad (1)$$

where
$p_i \in P$ the predicted binary segmentation
$g_i \in G$ – the ground truth binary volume

Binary Cross Entropy loss function has one advantage when compared to the other loss function. The gradient of the Binary cross entropy is smooth and hence a custom defined loss function Binary Cross Entropy with Dice loss is used.

$$L(y_{true}, y_{pred}) = BCE + (1 - D) \quad (2)$$

Where

$$BCE\ Loss = -\frac{1}{N}\sum_{n=1}^{N}[y_n \log \hat{y}_n + (1 - y_n)\log(1 - \hat{y}_n)]\ \text{Loss=-1/N\_n=1\^{}N?y\_nlogy\_n+1-y\_nlog1-y\_n} \quad (3)$$

c. Evaluation Metric - Mean IoU

The IoU which is also known as Jaccard Index is used in our experiments to estimate the percentage of overlap between the predicted binary output and binary ground truth. IoU is closely associated with the Dice coefficient which is used as a part of loss function. In simple terms IoU is the ratio between the number of common pixels between predicted and target output and total number of pixels present in both binary masks.

$$IoU = \frac{target \cap prediction}{target \cup prediction} \quad (4)$$

d. Estimation of Area and Perimeter of Nuclei

The segmented images are further processed to estimate the area and perimeter of the nuclei to analyse the growth of the cancerous cells at different stages of the disease. Freeman chain coding is adopted to represent the segmented nuclei in the binary object [15]. The coding uses a three bit code $0 \leq c \leq 7$ for each point in the contour of the nuclei region. The number c denotes the direction of the next boundary point. 8-connected freeman coding approach is employed and the boundary chain codes are determined using a traversing process which requires $O(N)$ operations where N is the length of the code. The area of a nuclei region represented using Freeman chain codes c1 c2….cn can be calculated using the mathematical expression given below.

$$A = \sum_{i=1}^{n} c_{ix} \left(y_{i-1} + \frac{c_{iy}}{2} \right) \qquad (5)$$

Where 'n' is the length of the chain and c_{ix} & c_{iy} are the **x** and **y** components of i^{th} chain element. The values of c_{ix} and c_{iy} belongs to {1, 0, -1} which indicates the change of the **x** and **y** coordinates. The perimeter of the nuclei region can be calculated using

$$P = n_e + \sqrt{2} n_o \qquad (6)$$

Where n_e and n_o represents the number of even and odd chain elements.

IV.EXPERIMENT AND RESULTS

The nuclei segmentation problem may seem to be kind of semantic segmentation problem but in fact it is instance segmentation where each nucleus in the image is independent of the other nuclei. The main objective of this segmentation is to track the size, the volume and the structure of the nuclei present in the cell over a period of time. In the experiments three deep learning models namely deep CNN, U-Net, and LinkNet have been trained and tested on the chosen dataset.

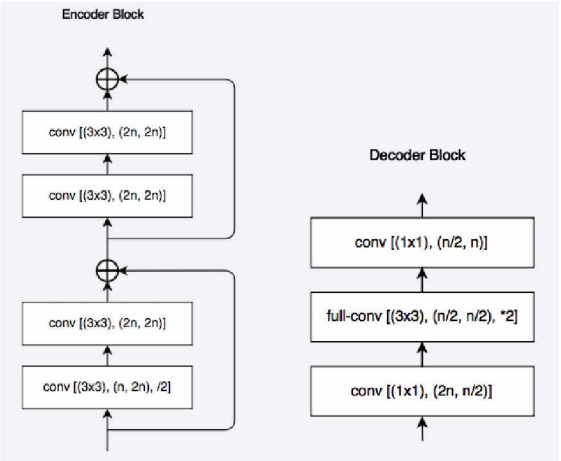

Fig. 7. Architecture of Encoder and Decoder Block in LinkNet

Mask-RCNN is not used in the experiments since it is hard to train the model with a two stage process. In the first stage regional proposal network is optimized and then in the second stage bounding boxes, classes and a binary mask are generated. The structure of encoder and decoder block and the architecture of the ResNet-18 used to construct the encoder block is shown in Figure 7. The first encoder block performs a non-strided convolution and output of each convolutional layer is given to a batch normalizer and ReLu activation function.

The main advantage of using a U-Net architecture based model when compared to a fully convolutional neural network is that during up-sampling the high resolution features are extracted which helps to better localize and learn representation. But the U-Net model suffers from another problem that it has generated a combined mask for many nuclei and they appear to be either overlapping or very close to each other. LinkNet-34 architecture efficiently transfers the information extracted in the encoder block to the corresponding decoder block after down-sampling the image. This makes the LinkNET more accurate than the fully convolutional network or network with pooled indices in the decoder block. This makes the number of parameters in the decoding block lesser. Figure 8 presents the comparison of segmentation results of CNN, U-NET, and Link-NET architecture.

Table I: Validation Results

Model	IoU	Dice Coefficient	Accuracy
CNN	83.6	0.82	92.1
U-Net	86.2	0.86	94.8
LinkNet	89.8	0.89	97.2

V.CONCLUSION

This paper proposed a deep learning based approach for cell nuclei semantic segmentation in histopathology images of breast cancer. The network structure consists of three parts: downsampling module, upsampling module, and links connecting the downsampling and upsampling blocks respectively. The links connecting the respective downsampling and upsampling layers helps to preserve the spatial information lost during the downsampling process. The model shows superior performance over the fully convolutional neural network as during upsampling more features are extracted which better localize and learn representation perfectly. Binary cross entropy and dice coefficient are combined used as loss function and the network is optimized using Adam optimizer. The Adam optimizer helps to converge quickly and improves the overall segmentation accuracy of the model. The methods used for estimation of area and perimeter of the nuclei region found to be less complex and accurate.

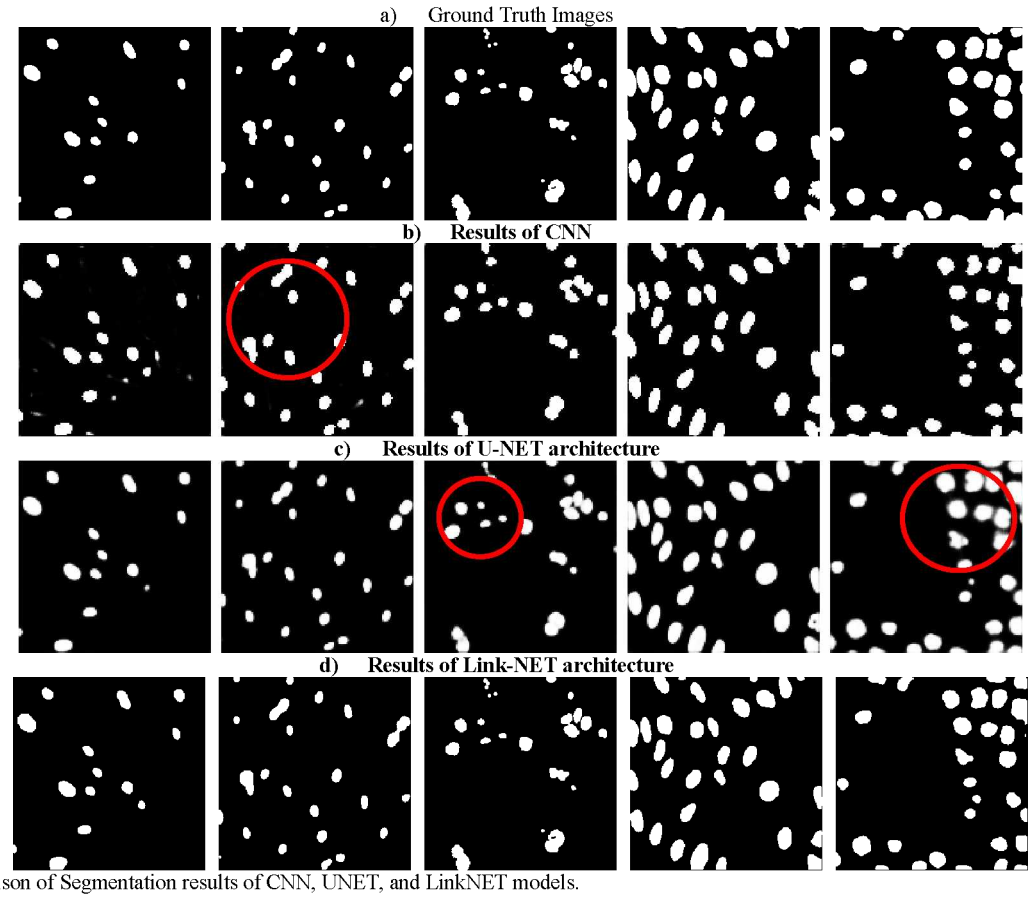

Fig. 8. Comparison of Segmentation results of CNN, UNET, and LinkNET models.

REFERENCES

[1] S. Malvia, S. A. Bagadi, U. S. Dubey, and S. Saxena, "Epidemiology of breast cancer in Indian women: Breast cancer epidemiology", Asia-Pacific J. Clin. Oncol., Vol. 13, No. 4, pp. 289-295, 2017.

[2] M. Veta, J. P. W. Pluim, P. J. van Diest and M. A. Viergever, "Breast Cancer Histopathology Image Analysis: A Review," in IEEE T Biomed. Eng., vol. 61, no. 5, pp. 1400-1411, 2014.

[3] J. S. Meyer, C. Alvarez, C. Milikowski, N. Olson, I. Russo, J. Russo, A. Glass, B. A. Zehnbauer, K. Lister, and R. Parwaresch, "Breast carcinoma malignancy grading by bloom–richardson system vs proliferation index: Reproducibility of grade and advantages of proliferation index," Mod. Pathol., vol. 18, no. 8, pp. 1067–1078, 2005.

[4] E. A. Perez, V. J. Suman, N. E. Davidson, S. Martino, P. A. Kaufman, W. L. Lingle, P. J. Flynn, J. N. Ingle, D. Visscher, and R. B. Jenkins, "HER2 testing by local, central, and reference laboratories in specimens from the north central cancer treatment group N9831 intergroup adjuvant trial," J. Clin. Oncol., vol. 24, no. 19, pp. 3032–3038, 2006.

[5] I. Pöllänen, B. Braithwaite, K. Haataja, T. Ikonen and P. Toivanen, "Current analysis approaches and performance needs for whole slide image processing in breast cancer diagnostics," 2015 International Conference on Embedded Computer Systems: Architectures, Modeling, and Simulation (SAMOS), Samos, pp. 319-325, 2015.

[6] P. Wang et al., "Automatic cell nuclei segmentation and classification of breast cancer histopathology images," Sig. Proc., Vol. 122, pp. 1–13, 2016.

[7] M. E. Plissiti, C. Nikou and A. Charchanti, "Automated detection of cell nuclei in Pap smear images using morphological reconstruction and clustering," IEEE T. Inf. Technol. Biomed. Vol. 15, No.2, pp.233–241, 2010.

[8] O. Ronneberger, P. Fischer, and T. Brox, "U-net: Convolutional networks for biomedical image segmentation," in International Conference on Medical Image Computing and Computer-Assisted Intervention. Springer, pp. 234–241, 2015.

[9] J. W. Johnson, "Adapting Mask-RCNN for Automatic Nucleus Segmentation", arXiv: 1805.00500v1, 2018.

[10] A. Chaurasia, and E. Culurciello, "Linknet: Exploiting encoder representations for efficient semantic segmentation", arXiv preprint arXiv:1707.03718, 2017.

[11] K. He, X. Zhang, S. Ren, and J. Sun, "Deep residual learning for image recognition", In: Proceedings of the IEEE conference on computer vision and pattern recognition, pp. 770–778, 2016.

[12] https://www.kaggle.com/c/data-science-bowl-2018/data

[13] K. He, et al, "Deep residual learning for image recognition." Proceedings of the IEEE conference on computer vision and pattern recognition. 2016.

[14] V. Badrinarayanan, A. Handa, and R. Cipolla, "Segnet: A deep convolutional encoder-decoder architecture for robust semantic pixel-wise labelling," arXiv preprint arXiv:1505.07293, 2015.

[15] H. Freeman, "Boundary encoding and processing", In B. S. Lipkin and A. Rosenfeld, editors, Picture Processing and Psychopictorics, pp.241-266, 1970.

[16] A. Shvets, et al, "Automatic instrument segmentation in robot-assisted surgery using deep learning." 2018 17th IEEE International Conference on Machine Learning and Applications (ICMLA). IEEE, 2018.

[17] S. Almutairi, S. Manimurugan, and M. Aborokbah, "A new secure transmission scheme between senders and receivers using HVCHC without any loss." EURASIP Journal on Wireless Communications and Networking, Vol. 88, 2019.

[18] S. Manimurugan., K. Porkumaran., and C. Narmatha, "The New Block Pixel Sort Algorithm for TVC Encrypted Medical Image", Imag. Sci. J, Vol. 62 No.8, PP. 403-414, 2014.

[19] C. Narmatha, P. Manimegalai, and S. Manimurugan, "A Grayscale Image Hiding Encode Scheme for Secure Transmission", Curr. Sig. Transd. Ther., Vol.14, Number 2, pp. 146-151, 2019.